

# Swimming Efficiently by Wrapping

H. Gidituri<sup>1</sup> and M. Ellero<sup>1,2,3</sup> and F. Balboa Usabiaga<sup>1†</sup>

<sup>1</sup>BCAM - Basque Center for Applied Mathematics, Alameda de Mazarredo 14, E48009 Bilbao, Basque Country - Spain

<sup>2</sup>Ikerbasque, Basque Foundation for Science, Calle de Maria Diaz de Haro 3, E48013 Bilbao, Basque Country - Spain

<sup>3</sup>Zienkiewicz Center for Computational Engineering (ZCCE), Swansea University, Bay Campus, Swansea SA1 8EN, UK

(Received xx; revised xx; accepted xx)

Single flagellated bacteria are ubiquitous in nature. They exhibit various swimming modes using their flagella to explore complex surroundings such as soil and porous polymer networks. Some single-flagellated bacteria swim with two distinct modes, one with its flagellum extended away from its body and another with its flagellum wrapped around it. The wrapped mode has been observed when the bacteria swim under tight confinements or in highly viscous polymeric melts. In this study we investigate the hydrodynamics of these two modes inside a circular pipe. We find that the wrap mode is slower than the extended mode in bulk but more efficient under strong confinement due to a hydrodynamic increased of its flagellum translation-rotation coupling.

## 1. Introduction

Bacteria are prokaryotic microorganisms forced to live in a zero Reynolds number environment. Due to the kinematic reversibility of viscous flows, some bacteria have developed a non-reciprocal propulsion mechanism for locomotion, the rotation of flagella. The cell body and the flagella are rotated in opposite directions by molecular motors. Under rotation the flagella adopt an helical shape and propel the bacterium by working as a screw. Some bacteria can move both forward or backward, in a push or pull mode, depending on the direction of rotation of the molecular motors and on the chirality of their flagella. As bacteria are often found in confined environments they have developed different strategies to swim while foraging in those conditions. One example is a swimming mode used by some monotrichous and bipolar bacteria where bacteria wrap their flagella around their own bodies resembling an Archimedes' screw Kühn *et al.* (2017); Tian *et al.* (2022); Thormann *et al.* (2022). These bacteria swim alternating between two different modes, the wrapped mode and the extended mode, where the later has the flagella extended away from their bodies.

The wrap mode emerges when a cell encounter highly viscous or strongly confined environments Kühn *et al.* (2017). When a cell gets trapped during its forward pushing mode a buckling instability occurs in the flagellar hook that triggers the flagellum wrapped mode Kühn *et al.* (2017); Park *et al.* (2022). The number of known bacterial species showcasing a wrap mode under confinement is growing Thormann *et al.* (2022). Thus, a natural question arises: is the wrapped mode a mere accident or is it selected due to some advantage to the bacteria? Some studies suggest that the wrapped mode confer advantages to the motion in confinement environments. Kühn *et al.* observed experimentally that the wrapped mode can enhance the motion in highly viscous and

† Email address for correspondence: fbalboa@bcamath.org

structured environments Kühn *et al.* (2018). Kinosita *et al.* studied the motion of bacteria with wrapped mode in very tight confinements and concluded that the wrapped mode can allow the bacteria to glide over the substrate Kinosita *et al.* (2018). Along this line of work we investigate how the flagella motion in the wrapped mode favors the motion of bacteria under strong confinement by hydrodynamic interactions only. To this end we investigate the swimming of bacteria inside circular pipes by means of CFD simulations. We show that the extended mode is more efficient in bulk and wide pipes while the wrapped mode can be more efficient in tight pipes. The scheme of the paper is the following. In Sec. 2 we describe our numerical method, describe our results in Sec. 3 and conclude in Sec. 4.

## 2. Numerical Method

We model a monotrichous bacterium as a rigid ellipsoid with an helical flagellum attached to one of its poles. The flagellum is also modeled as a rigid object, which is a good approximation to study steady state swimming Higdon (1979); Das & Lauga (2018). The body and the flagellum are connected by inextensible links that allow the flagellum to rotate freely around its main axis but otherwise it is forced to move concomitant to the rigid ellipsoid. The rigid objects,  $\mathcal{B}_n$ , move with linear and angular velocities,  $\mathbf{u}_n$  and  $\boldsymbol{\omega}_n$ , where we use the subindex  $n$  to denote either the bacterium body or the flagellum. Due to the small bacterium size, the flow Reynolds number is vanishingly small,  $\text{Re} \sim 10^{-5}$ . Thus, the flow can be modeled with the Stokes equations

$$-\nabla p + \mu \nabla^2 \mathbf{v} = \mathbf{0}, \quad (2.1)$$

$$\nabla \cdot \mathbf{v} = 0, \quad (2.2)$$

where  $p$  and  $\mathbf{v}$  are the fluid pressure and velocity and  $\mu$  its viscosity. The no-slip boundary condition is imposed on the surface of the bacterium body and its flagellum

$$\mathbf{v}(\mathbf{r}) = \mathbf{u}_n + \boldsymbol{\omega}_n \times (\mathbf{r} - \mathbf{q}_n) \quad \text{for } \mathbf{r} \text{ on the bacterium,} \quad (2.3)$$

where  $\mathbf{q}_n$  is tracking point of the rigid bodies (e.g. the bacterium body center and the flagellum attaching point respectively).

To solve the coupled fluid-structure interaction problem we use the rigid multiblob method for articulated bodies. We summarized the numerical method while a detailed description can be found elsewhere Balboa Usabiaga & Delmotte (2022). The rigid bodies are discretized with a finite number of *blobs* with position  $\mathbf{r}_i$  as shown in Fig. 1. As the inertia is negligible the conservation of momentum reduces to the balance of force and torque. The discrete force and torque balance for the rigid object  $n$  can be written as,

$$\sum_{i \in \mathcal{B}_n} \boldsymbol{\lambda}_i - \sum_{i \in \mathcal{L}_n} \boldsymbol{\phi}_n = \mathbf{f}_n, \quad (2.4)$$

$$\sum_{i \in \mathcal{B}_n} (\mathbf{r}_i - \mathbf{q}_n) \times \boldsymbol{\lambda}_i - \sum_{i \in \mathcal{L}_n} (\Delta \mathbf{l}_{np} - \mathbf{q}_n) \times \boldsymbol{\phi}_n = \boldsymbol{\tau}_n, \quad (2.5)$$

where  $\mathbf{f}_n$  and  $\boldsymbol{\tau}_n$  are the external forces and torques acting on the rigid objects while  $\boldsymbol{\lambda}_i$  are the constrained forces acting on the blobs that ensure the rigid motion of the bacterium body and the flagellum. The second sums in (2.4)-(2.5) run over the links,  $\mathcal{L}_n$ , attached to the rigid object  $n$  and  $\boldsymbol{\phi}_n$  is the force exerted by the link  $n$  to keep the rigid bodies connected while  $|\Delta \mathbf{l}_{np}|$  is the link length.

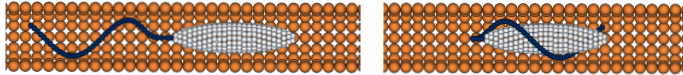


FIGURE 1. Bacteria,  $2.04\ \mu\text{m}$  long and  $0.49\ \mu\text{m}$  wide, inside a pipe with its flagellum in the extended and wrapped configuration. The front of the pipe is not shown to make the bacteria visible.

The discrete no-slip condition evaluated at each blob  $i$  is,

$$\mathbf{v}(\mathbf{r}_i) = \sum_j \mathbf{M}_{ij} \boldsymbol{\lambda}_j = \mathbf{u}_n + \boldsymbol{\omega}_n \times (\mathbf{r}_i - \mathbf{q}_n) \quad \text{for } i \in \mathcal{B}_n. \quad (2.6)$$

The mobility matrix  $\mathbf{M}_{ij}$  gives the hydrodynamic interaction between any two blobs,  $i$  and  $j$ , of radius  $a_i$  and  $a_j$ . We use a regularized version of the Oseen tensor, the Rotne-Prager tensor, Wajnryb *et al.* (2013).

$$\mathbf{M}_{ij} = \frac{1}{(4\pi a_i a_j)^2} \int \delta(|\mathbf{r}' - \mathbf{r}_i| - a_i) \mathbf{G}(\mathbf{r}', \mathbf{r}'') \delta(|\mathbf{r}'' - \mathbf{r}_j| - a_j) d^3 r' d^3 r'', \quad (2.7)$$

where  $\mathbf{G}(\mathbf{r}, \mathbf{r}')$  is the Green's function of the Stokes equation and  $\delta(r)$  the Dirac's delta function. The advantage of this formulation is that the regularized mobility has no divergence even when blobs get close and it is not necessary to use special quadrature rules. The equations (2.4)-(2.6) form a linear system for the unknown velocities,  $\mathbf{u}_n$  and  $\boldsymbol{\omega}_n$ , and constraint forces,  $\boldsymbol{\lambda}_j$  and  $\boldsymbol{\phi}_n$ , that can be solved efficiently with iterative methods such as GMRES Balboa Usabiaga *et al.* (2016); Balboa Usabiaga & Delmotte (2022).

### 3. Results and Discussion

In this section we study the swimming of bacteria inside circular pipes of radius  $r_0$  and length  $L_0 \approx 21r_0$  aligned along  $z$ . Keeping the aspect ratio constant ensures that the flow disturbance created by a bacterium decays to negligible values at the pipes ends Liron & Shahar (1978). We model the pipes as immobile rigid objects Balboa Usabiaga *et al.* (2016). We place the bacteria in the middle of the pipes and we use that configuration to compute the bacteria velocity. As the Stokes equation assume a steady state flow solving one mobility problem is enough to determine the velocities. Later, we will consider the case where bacteria freely swim in a pipe periodic along its main axis.

We consider two different swimming modes. First, the extended mode where the flagellum is attached to the body front part and it extends away from it. In the second mode the flagellum is wrapped around the bacteria body, see Fig. 1. In both cases we apply constant and opposite torques, of magnitude  $\tau = 0.46\ \text{pN}\mu\text{m}$ , to the body and the flagellum to model the work exerted by a molecular motor. Thus, we assume that the molecular motor always works on the low frequency (constant torque) regime Xing *et al.* (2006). In most numerical experiments the flagellum extends along its main axis a length similar to the bacterium body. Thus, in the wrapped mode the body is fully covered by the flagellum. The bacterium body, always  $2.04\ \mu\text{m}$  long and  $0.49\ \mu\text{m}$  wide, is discretized with 292 blobs of radius  $a = 0.0425\ \mu\text{m}$ . The geometric details of the helical flagella and pipes used in this work are presented in Tables 1 and 2.

All the motion is driven by the rotation of the flagellum. Therefore, we start looking at its angular velocity,  $\omega_z$ , see Fig. 2a. In bulk the flagellum rotates two times faster in the extended mode than in the wrapped mode. The slower rotation can be explained by the additional drag experienced by the flagellum in the wrapped mode, which is caused by the proximity of the flagellum to the bacterium body. Both modes reduce their angular

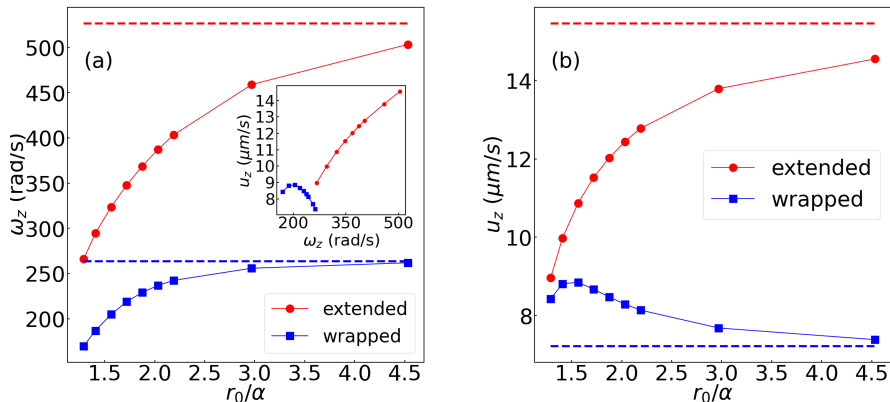


FIGURE 2. Flagellum angular velocity,  $\omega_z$ , (a) and bacterium swimming speed along the pipe,  $u_z$ , (b) versus pipe radius  $r_0$ . Results for the extended and wrapped mode using the same flagellum (model VII) with length  $L = 3.6, \mu\text{m}$  and amplitude  $\alpha = 0.32 \mu\text{m}$ . The dashed lines depict bulk values. The inset in the right panel shows the swimming speed against the flagellum angular frequency for all the pipe radius used.

velocities as  $r_0$  decreases due to the additional hydrodynamic drag generated by the pipe walls. However, the decrease is proportionally less important in the wrapped mode as its initial drag was larger. Thus, the ratio between the angular frequencies of the two modes falls from a factor 2.0 in bulk to a factor 1.6 in the smallest pipe considered.

Next, we look at the swimming speed along the pipe axis,  $u_z$ , see Fig. 2b. We observe that in bulk the wrapped mode swims about twice slower than the extended mode. This result is consistent with experimental observations Kühn *et al.* (2017); Tian *et al.* (2022); Grognot & Taute (2021); Thormann *et al.* (2022). The slower swimming speed in the wrapped mode is a consequence of the slower rotation of its flagellum. Under confinement the swimming speed,  $u_z$ , decreases for the extended mode as the pipe radius is decreased. Again, the additional hydrodynamic drag generated by the pipe walls is responsible for this effect. In contrast, the wrapped mode exhibits a non-monotonic trend in its swimming speed. As the pipe radius is decreased the bacterium swims faster up to the point where the ratio between the pipe radius and the flagellum amplitude is  $r_0/\alpha \approx 1.5$ . Beyond that point the swimming speed decreases with  $r_0$ .

The Stokes equations are linear and thus the linear and angular velocity are proportional when keeping all geometric parameters constant. We could have imagined that changing the pipe radius would affect the flagellum rotation and the bacterium translation to a similar degree. That is approximately true for the extended mode but completely false for the wrapped mode as shown in the inset of Fig. 2a. To understand this difference and the unusual swimming speed increase observed with the wrapped mode we consider the motion of a single helical flagellum inside a pipe. We apply a constant torque on the helical flagellum and measure its translational and rotational speeds. Note that in this case the flagellum is not a torque-free swimmer, as there is no body to which apply an opposite torque. Nonetheless, this numerical experiment is useful to understand the more complex wrapped mode. We observe an increase in the swimming speed for decreasing pipe radius with respect to the bulk value above a critical pipe radius, see Fig. 3a, similar to the wrapped mode results. For the single flagellum its swimming speed can be written as  $u_z = M_{tr}\tau_z$ . For moderate confinements

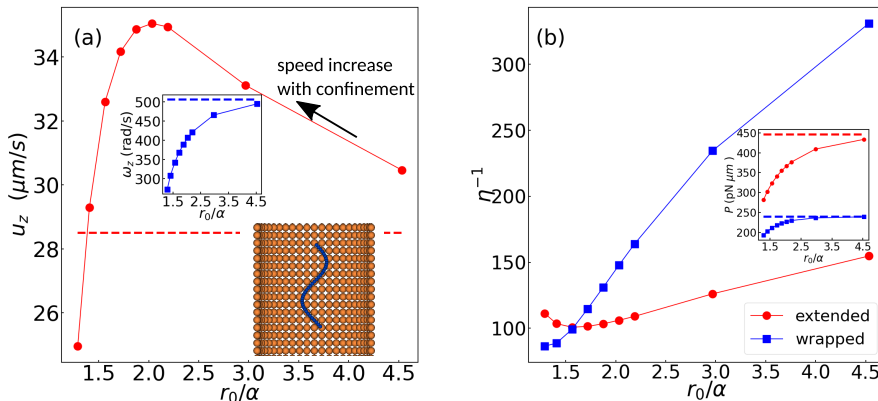


FIGURE 3. (a) Swimming speed,  $u_z$ , and z-component of the angular velocity (inset),  $\omega_z$ , of a single helical flagellum with amplitude  $\alpha = 0.32 \mu\text{m}$  (model VII) inside a pipe of radius  $r_0$ . The dashed lines depicts the bulk values and a snapshot of the flagellum in a pipe is shown as inset. (b) Inverse of the efficiency versus radius of the pipe ( $r_0$ ). The dashed lines depicts the bulk values. The inset figure shows the swimming power.

the hydrodynamic interactions with the wall increase the value of the mobility coupling term,  $M_{tr}$ , with respect to the bulk values, thus, the swimming speed is increased. For very tight confinements the lubrication interactions dominate the interactions with the wall and  $M_{tr}$  decreases below the bulk values. These effects were already reported by Liu *et al.* for an infinite flagellum within an infinite pipe Liu *et al.* (2014). This speed increase is observed despite the reduction in the flagellum angular velocity,  $\omega_z$ , with  $r_0$ , see Fig. 3a inset. The wrapped mode takes advantage of the increased translation-rotation coupling of its flagellum under confinement to increase its speed. In the extended mode the flagellum translation-rotation coupling is increased just as in the wrapped mode. However, the drag on the body increases faster with smaller  $r_0$ , the combined effect is to reduce the swimming speed. In the wrapped mode the body is protected by the flagellum, moving in the same direction, and thus the increase in the body drag is less important.

This interplay between the enhanced translation-rotation coupling, which increases thrust and the swimming speed, and the drag on the bacterium body which reduces it, has been observed in a recent experimental study with *E. coli* Vizsnyiczai *et al.* (2020). Vizsnyiczai *et al.* observed that a bacterium swimming in a extended mode inside a pipe swims slower than a bacterium in a channel. However, when the bacterium is exiting the pipe and only its flagella remain inside, the swimming speed is larger than a channel. The reason is the increased translation-rotational coupling experienced by the flagella and the lack of an additional drag acting on the bacterium body. This result was nicely reported in Fig. 5 of Ref. Vizsnyiczai *et al.* (2020). After the flagella exit the pipe the speed decreases to the bulk value. Our results agree with their observations.

### 3.1. Power and Efficiency

The power consumption is an important quantity for a microswimmer propelling in a viscous environment and the efficiency can be more important than the absolute swimming speed. Thus, we measure these quantities. Considering the chemical energy used within the cell is beyond the scope of our work, thus, we limit ourselves to study the power dissipated by the Stokes flow and the microswimmers hydrodynamic efficiency.

---

Model	$L$ [ $\mu\text{m}$ ]	$\alpha$ [ $\mu\text{m}$ ]	$k$ [ $\mu\text{m}^{-1}$ ]	$L_z$ [ $\mu\text{m}$ ]	$N_\lambda$	$a$ [ $\mu\text{m}$ ]	$N_b$
I	3.2938	0.32	2.2656	2.5681	0.8	0.0425	40
II	3.5372	0.32	2.8280	2.5681	1.0	0.0425	45
III	4.2737	0.32	4.2500	2.5681	1.5	0.0425	52
IV	5.1058	0.32	5.6562	2.5681	2.0	0.0425	60
V	5.9953	0.32	7.0625	2.5681	2.5	0.0425	72
VI	5.1747	0.32	2.8280	3.8414	2.83	0.0425	69
VII	3.6783	0.32	3.1250	2.3982	1.1	0.0425	43

---

TABLE 1. Flagella models parameters. Flagella length,  $L$ , amplitude,  $\alpha$ , wave number,  $k$ , maximum extension along its axis,  $L_z$ , number of waves along its axis,  $N_\lambda = L_z/\lambda = L_z k/(2\pi)$ , blob radius,  $a$ , and number of blobs  $N_b$ . The amplitude of the wave was exponentially damped near the attaching point with a damping factor  $k_E = k$  as in Ref. Higdon (1979).

---



---

Model	$L$ [ $\mu\text{m}$ ]	$r_0$ [ $\mu\text{m}$ ]	$N_b$	Model	$L$ [ $\mu\text{m}$ ]	$r_0$ [ $\mu\text{m}$ ]	$N_b$
I	9.35	0.4125	720	VI	14.1	0.65	1562
II	10.1	0.45	816	VII	15.1	0.7	1824
III	11.1	0.50	1008	VIII	20.1	0.95	3232
IV	12.1	0.55	1159	IX	30.1	1.45	7248
V	13.1	0.60	1386				

---

TABLE 2. Pipes models dimensions. Length,  $L$ , inner radius  $r_0$ , number of blobs  $N_b$ . The blob radius is  $a = 0.1 \mu\text{m}$  in all cases.

---

The power exerted by a microswimmer to the medium and dissipated by the flow is

$$P = \sum_n \mathbf{F}_n \cdot \mathbf{U}_n = \sum_n [\mathbf{f}_n \cdot \mathbf{u}_n + \boldsymbol{\tau}_n \cdot \boldsymbol{\omega}_n], \quad (3.1)$$

where the sum is over rigid bodies, in our case the bacterium body and its flagellum. As the power is generated by the motor, the power consumed by a bacteria during its swimming can be rewritten as  $P_m = \boldsymbol{\tau}_m \cdot \boldsymbol{\omega}_m = \boldsymbol{\tau}_m \cdot (\boldsymbol{\omega}_{\text{flag}} - \boldsymbol{\omega}_{\text{body}})$ . In the absence of elastic or soft steric interactions both expressions are equivalent. We will always use (3.1) to account for soft steric interactions used in Sec. 3.3.

The wrapped mode consume less power for all pipe radii owing to the slower rotation of its flagellum, see Fig. 3b inset. Under confinement the power exerted by the motor decays for both swimming modes. Of more interest is the hydrodynamic efficiency of the swimmers to propel themselves. There are several approaches to define the hydrodynamic efficiency Childress (2012). We follow a classical approach and define the inverse efficiency as the power normalized with the power necessary to pull the body with the same speed Higdon (1979); Lauga & Eloy (2013)

$$\eta^{-1} = \frac{M_{zz}}{u_z^2} P, \quad (3.2)$$

where  $M_{zz} = u_z/f_z$  is body mobility along the pipe axis and  $u_z$  the velocity. The Fig. 3b shows the variation of the inverse efficiency as a function of the pipe radius. It is evident from the figure that in bulk and wide pipes the extended mode is more efficient. However, there is a crossover and for tight confinements the wrapped mode becomes more efficient. This is a result of the lower power consumption of the wrapped mode and, importantly,

its enhanced velocity within the pipe. This result suggest that the wrapped mode is beneficial to selfpropel in confined spaces. So far we have only used one flagellum, model II, and a bacterium placed exactly on the middle of the pipe. In the next two sections we explore whether these results are robust under a change of these conditions.

### 3.2. Robustness of results: Effect of $N_\lambda$ and $L$

Bacteria species present flagella of different lengths, amplitudes and pitch angles which affect the bacteria bulk speeds and efficiencies Higdon (1979); Lauga & Eloy (2013). Here, we explore if the wrapped mode is a more efficient swimming style in confined environments for a wide variety of flagella models. We build five flagella models by varying simultaneously the flagellum length,  $L$ , and the number of waves along its length,  $N_\lambda = L_z/\lambda$ , where  $L_z$  is the flagellum extension along its axis and  $\lambda$  the wavelength of the helical wave, see Fig. 4(a,b) and Table 1. We present the inverse efficiency for all flagella models and pipe radius in Fig. 4(c,d)

The general trend is the same as before. For wide pipes the extended mode swims more efficiently than the wrapped mode for all flagella models except one ( $N_\lambda = 2.5$ ). Under confinement both swimmers increase their efficiency but the improvement is stronger for the wrapped mode which becomes the most efficient for pipes with  $r_0/\alpha \lesssim 1.7$ . In those situations the wrapped mode is approximately two times more efficient than the extended mode. The efficiency, for both swimming modes, is non-monotonous on  $N_\lambda$ . When  $N_\lambda \ll 1$  the flagellum is almost straight, thus, it cannot propel the bacterium. Therefore, the swimming speed and the efficiency initially grow with  $N_\lambda$ . Beyond a certain value of  $N_\lambda$  the flagellum tangent forms a large angle with the direction of motion, which again reduces the propulsion efficiency. For intermediate values of  $N_\lambda$  the flagellum is helical-shaped which allows propulsion. For both modes the flagellum with  $N_\lambda = 1.5$  is the most efficient under confinement for the flagella lengths considered. For bacteria swimming in bulk the optimum is also close to  $N_\lambda = 1.5$ , although the exact optimum  $N_\lambda$  depends on the flagellum length Higdon (1979). For the extended mode, optimal swimming occurs around the non-dimensional pipe radius,  $r_0/\alpha = 1.5$  for all values of  $N_\lambda$ . For the wrap mode the optimal swimming occurs for lower values of  $r_0/\alpha$ .

### 3.3. Robustness of results: dynamical simulations

So far we have computed the swimming speed when the bacteria are located in the middle of the pipe and aligned along it. However, freely swimming bacteria can tilt and move towards the pipe wall. To verify if the results reported so far are robust, we perform dynamic simulations where the bacteria are free to displace away from the pipe centerline and to change orientations. We use the same pipe models as before but imposing periodic boundary conditions along the pipe. To solve the Stokes equations with these boundary conditions we use a periodic Fast Multipole Method implemented in the library STKFMM Yan & Shelley (2018). To avoid the overlap of the bacterium with the pipe we include a steric repulsion interaction between the blobs of pipe and bacterium with a repulsion strength  $f = 5 \times 10^{-5} \text{pN}\mu\text{m}$  for overlapping blobs and with an exponential decay with a characteristic length  $\xi = 0.01 \mu\text{m}$  for non-overlapping blobs.

For all models considered in this section we simulate the bacteria for 10 s so the bacteria can swim at least  $70 \mu\text{m}$ . We use the last 8 s to extract the swimming speed and the power consumption. The results for bacteria with the flagella model VII, the one used in Fig. 2, are shown as full symbols in Fig. 5. The same general trend as for the static simulations is observed. However, the efficiency curves do not cross over. The cross over is not observed because this time the wrapped swimming speed along the pipe,  $u_z$ , barely increases with

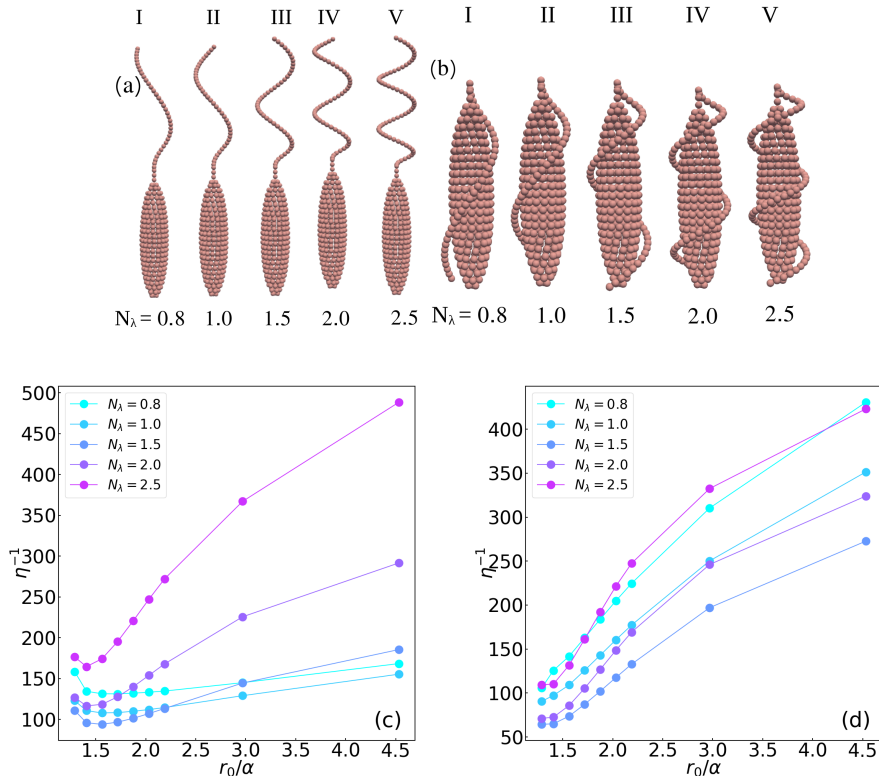


FIGURE 4. Shapes of extended **(a)** and wrapped **(b)** bacteria modes with different  $N_\lambda$  values. Inverse of the swimming efficiency versus radius of the pipe ( $r_0$ ) for different values of  $N_\lambda$  for the extended mode **(c)** and the wrapped mode **(d)**.

confinement, and the efficiency depends strongly on  $u_z$ . The magnitude of  $u_z$  does not increase because the bacterium swims with a tilt towards the wall, see Fig. 5c and Movie 1. In contrast, the extended mode cannot tilt significantly on small pipes as that is prevented by its rigid flagellum, which favours the motion along the pipe.

To verify the role of the tilt we run another set of simulations using a longer flagellum, model VI, that extends beyond the bacterium body, see Fig. 5c and Movie 2. The results are presented as open symbols in Fig. 5. In this case the speed of the wrapped mode is approximately independent on the confinement but larger than with the shorter flagellum. As a result we observe a crossover between the efficiencies of the wrapped and extended modes. Overall, these results show that *(i)* the swimming speed is less sensitive to confinement for the wrapped mode than for the extended mode, *(ii)*, the efficiency improves strongly for the wrapped mode and *(iii)*, depending on the flagellum details, the wrapped mode can be the most efficient way to swim.

#### 4. Conclusions

In this paper we have presented the dynamics of two different swimming modes, namely the extended and wrapped modes of monotrichous type bacteria. Under bulk conditions the extended mode swims faster and more efficiently than the wrapped mode. However, under strong confinement the efficiency of the wrapped mode improves faster than for the extended mode. For a wide number of flagella shapes, with different lengths and

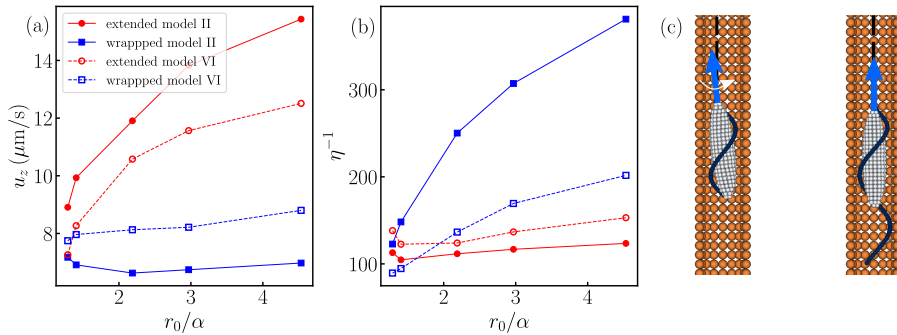


FIGURE 5. Swimming speed (a) and hydrodynamic efficiency (b) of wrapped and extended modes swimming a long a periodic pipe extracted from 10s long dynamic simulations. Full symbols use flagellum model VII, which extends the same length as the body, and open symbols use model flagellum VI, which extends longer. The longer flagellum prevents the tilt of the wrapped mode which results in higher speeds and better efficiencies. (c) Two bacteria inside a pipe. A bacterium with a short flagellum performs a precession motion around the pipe axis while a bacterium with a long flagellum is forced to swim straight. The swimming direction is shown with a short arrow and the pipe axis with a dashed line.

wavelengths, the bacteria in the wrapped mode swim more efficiently. These results are complementary to the experimental work of Kinosita *et al.* where the bacteria *Burkholderia* adopting the wrapped mode was observed to glide in very narrow ducts Kinosita *et al.* (2018). It seems that, either by gliding over a substrate or by means of hydrodynamic interactions, the wrapped mode promotes the motion of bacteria on tight confinements. It is interesting to note that some bipolar flagellated bacteria can display a wrapped and an extended mode simultaneously, where the flagellum at the front pole wraps around the body and the rear one remains extended Murat *et al.* (2015); Constantino *et al.* (2018); Thormann *et al.* (2022); Bansil *et al.* (2023). Such mixed mode could present some advantages under confinement that should be investigated.

## Acknowledgments

The project that gave rise to these results received the support of a fellowship from “la Caixa” Foundation (ID 100010434), fellowship LCF/BQ/PI20/11760014, and from the European Union’s Horizon 2020 research and innovation programme under the Marie Skłodowska-Curie grant agreement No 847648. Funding provided by the Basque Government through the BERC 2022-2025 program and by the Ministry of Science and Innovation: BCAM Severo Ochoa accreditation CEX2021-001142-S/MICIN/AEI/10.13039/501100011033 and the project PID2020-117080RB-C55 “Microscopic foundations of soft matter experiments: computational nano-hydrodynamics (Compu-Nano-Hydro)” are also acknowledged.

## REFERENCES

- BALBOA USABIAGA, FLORENCIO & DELMOTTE, BLAISE 2022 A numerical method for suspensions of articulated bodies in viscous flows. *Journal of Computational Physics* **464**, 111365.
- BALBOA USABIAGA, F., KALLEMOV, B., DELMOTTE, B., BHALLA, A. P. S., GRIFFITH, B. E. & DONEV, A. 2016 Hydrodynamics of suspensions of passive and active rigid particles: a rigid multiblob approach. *Communications in Applied Mathematics and Computational Science* **11** (2), 217–296.

- BANSIL, RAMA, CONSTANTINO, MAIRA A., SU-ARCARO, CLOVER, LIAO, WENTIAN, SHEN, ZELI & FOX, JAMES G. 2023 Motility of different gastric helicobacter spp. *Microorganisms* **11** (3).
- CHILDRESS, STEPHEN 2012 A thermodynamic efficiency for stokesian swimming. *Journal of Fluid Mechanics* **705**, 77–97.
- CONSTANTINO, MAIRA A, JABBARZADEH, MEHDI, FU, HENRY C, SHEN, ZELI, FOX, JAMES G, HAESBROUCK, FREDDY, LINDEN, SARA K & BANSIL, RAMA 2018 Bipolar lophotrichous helicobacter suis combine extended and wrapped flagella bundles to exhibit multiple modes of motility. *Scientific reports* **8** (1), 1–15.
- DAS, DEBASISH & LAUGA, ERIC 2018 Computing the motor torque of escherichia coli. *Soft Matter* **14**, 5955–5967.
- GROGNOT, MARIANNE & TAUTE, KATJA M 2021 More than propellers: how flagella shape bacterial motility behaviors. *Current Opinion in Microbiology* **61**, 73–81.
- HIGDON, J. J. L. 1979 The hydrodynamics of flagellar propulsion: helical waves. *Journal of Fluid Mechanics* **94** (2), 331–351.
- KINOSITA, YOSHIKI, KIKUCHI, YOSHITOMO, MIKAMI, NAGISA, NAKANE, DAISUKE & NISHIZAKA, TAKAYUKI 2018 Unforeseen swimming and gliding mode of an insect gut symbiont, burkholderia sp. rpe64, with wrapping of the flagella around its cell body. *The ISME journal* **12** (3), 838–848.
- KÜHN, MARCO J, SCHMIDT, FELIX K, ECKHARDT, BRUNO & THORMANN, KAI M 2017 Bacteria exploit a polymorphic instability of the flagellar filament to escape from traps. *Proceedings of the National Academy of Sciences* **114** (24), 6340–6345.
- KÜHN, MARCO J, SCHMIDT, FELIX K, FARTHING, NICOLA E, ROSSMANN, FLORIAN M, HELM, BINA, WILSON, LAURENCE G, ECKHARDT, BRUNO & THORMANN, KAI M 2018 Spatial arrangement of several flagellins within bacterial flagella improves motility in different environments. *Nature communications* **9** (1), 5369.
- LAUGA, ERIC & ELOY, CHRISTOPHE 2013 Shape of optimal active flagella. *Journal of Fluid Mechanics* **730**, R1.
- LIRON, N. & SHAHAR, R. 1978 Stokes flow due to a stokeslet in a pipe. *Journal of Fluid Mechanics* **86** (4), 727–744.
- LIU, BIN, BREUER, KENNETH S. & POWERS, THOMAS R. 2014 Propulsion by a helical flagellum in a capillary tube. *Physics of Fluids* **26** (1), 011701.
- MURAT, DOROTHÉE, HÉRISSE, MARION, ESPINOSA, LEON, BOSSA, ALICIA, ALBERTO, FRANÇOIS & WU, LONG-FEI 2015 Opposite and coordinated rotation of amphitrichous flagella governs oriented swimming and reversals in a magnetotactic spirillum. *Journal of Bacteriology* **197** (20), 3275–3282.
- PARK, JEUNGEUN, KIM, YONGSAM, LEE, WANHO & LIM, SOOKKYUNG 2022 Modeling of lophotrichous bacteria reveals key factors for swimming reorientation. *Scientific Reports* **12** (1), 6482.
- THORMANN, KAI M., BETA, CARSTEN & KÜHN, MARCO J. 2022 Wrapped up: The motility of polarly flagellated bacteria. *Annual Review of Microbiology* **76** (1), 349–367, PMID: 35650667.
- TIAN, MAOJIN, WU, ZHENGYU, ZHANG, RONGJING & YUAN, JUNHUA 2022 A new mode of swimming in singly flagellated pseudomonas aeruginosa. *Proceedings of the National Academy of Sciences* **119** (14), e2120508119.
- VIZSNYICZAI, GASZTON, FRANGIPANE, GIACOMO, BIANCHI, SILVIO, SAGLIMBENI, FILIPPO, DELL'ARCIPRETE, DARIO & DI LEONARDO, ROBERTO 2020 A transition to stable one-dimensional swimming enhances e. coli motility through narrow channels. *Nature communications* **11** (1), 2340.
- WAJNRYB, ELIGIUSZ, MIZERSKI, KRZYSZTOF A., ZUK, PAWEŁ J. & SZYMCZAK, PIOTR 2013 Generalization of the rotne–prager–yamakawa mobility and shear disturbance tensors. *Journal of Fluid Mechanics* **731**, R3.
- XING, JIANHUA, BAI, FAN, BERRY, RICHARD & OSTER, GEORGE 2006 Torque–speed relationship of the bacterial flagellar motor. *Proceedings of the National Academy of Sciences* **103** (5), 1260–1265.
- YAN, WEN & SHELLEY, MICHAEL 2018 Universal image system for non-periodic and periodic stokes flows above a no-slip wall. *Journal of Computational Physics* **375**, 263–270.